

OPEN ACCESS

Sub-wavelength ripple formation on various materials induced by tightly focused femtosecond laser radiation

To cite this article: Ralph Wagner and Jens Gottmann 2007 *J. Phys.: Conf. Ser.* **59** 333

View the [article online](#) for updates and enhancements.

You may also like

- [Pattern formation on Ge by low energy ion beam erosion](#)
Marc Teichmann, Jan Lorbeer, Bashkim Ziberi et al.
- [Carbon ion beam induced chemical modification and nano-pyramid growth on Si surface](#)
Sudip Bhowmick, Joy Mukherjee, Manorama Ghosal et al.
- [Surface nanopatterning by ion beam irradiation: compositional effects](#)
L Vázquez, A Redondo-Cubero, K Lorenz et al.



ECS
The
Electrochemical
Society
Advancing solid state &
electrochemical science & technology

DISCOVER
how sustainability
intersects with
electrochemistry & solid
state science research

Sub-wavelength ripple formation on various materials induced by tightly focused femtosecond laser radiation

Ralph Wagner, Jens Gottmann

Lehrstuhl für Lasertechnik, RWTH Aachen, Steinbachstraße 15, 52074 Aachen, Germany

E-mail: jens.gottmann@lt.rwth-aachen.de

Abstract. Sub-wavelength ripples ($<\lambda/4$) are obtained by scanning a tightly focused beam ($\sim 1\mu\text{m}$) of femtosecond laser radiation ($t_p=100\text{fs}$, $\lambda=800\text{nm}$ & 400nm) over the surface of various materials. The ripple pattern extends coherently over many overlapping laser pulses parallel and perpendicular to the polarisation. Investigated are the dependence of the ripple spacing Λ on the material. New results concerning the dependence of the spacing on the wavelength are presented. Some possible models for ripple growth are discussed and conditions under which these phenomena occur are contained. In opposition to the classical ripple theory, the observed ripple spacing is dependent on the material, giving indication to understand the processes during the sub-wavelength ripple formation by femtosecond laser radiation.

1. Introduction

Ripples or, named by the generic term, laser-induced periodic surface structures (LIPSS) have been observed substantially near the ablation threshold by many authors since the beginning of investigation of laser ablation four decades ago [1]. The great variety of experimental LIPSS was subsumed into theoretical approaches [2, 3, 4]. In the most common type of surface topography, a periodicity of about the wavelength λ of the laser radiation is observed. This has been attributed to interference between the incident laser radiation and scattered or excited surface waves [5]. Smaller and bigger spacing Λ between the ripples occur if the laser radiation has an inclination θ to the surface normal. The dependence $\Lambda = \lambda / (1 \pm \sin \theta)$ has been found, where the plus and the minus refer to the downwards and upwards running surface wave on the inclined surface [2]. In most cases the ripples orientation is found to be perpendicular to the incident polarisation. Because of the wide range of LIPSS, many other explanations have been considered [2, 6, 7, 8, 9].

Efforts were made to avoid ripples in microstructuring as their formation limits the precision of laser processing [10, 11, 4]. Otherwise it seems to be possible to utilize the ripples for micro and nano structuring [4], e.g. for fabrication of gratings [12] or waveguides in thin films [13]. Ripple structures created by femtosecond laser pulses have been reported [14, 15, 16]. Sub-wavelength ripple formation in different variations has been observed increasingly [17-23], but not investigated in detail, yet. Reproducible sub-wavelength ripples are presented with a structure size from $\Lambda = 1/4 * \lambda$ to $3/4 * \lambda$ depending on the irradiated material.

2. Experimental setup

Bulk materials structured are fused silica (FS, a-SiO₂), lithium fluoride (LiF), magnesium fluoride (MgF₂), sapphire (Al₂O₃), polytetrafluoroethylene (PTFE), silicon (Si) and ZBLAN, a multi-component fluoride glass [23]. The surfaces are polished and cleaned in an ultrasonic bath of ethanol before processing, so that no structures are detectable by light-optical microscopy.

Irradiation is carried out with a femtosecond CPA-laser system at a central wavelength of $\lambda=800\text{nm}$ and using a pulse duration of $t_p=100\text{fs}$ (FWHM). The spatial profile of the beam is nearly Gaussian. The laser is running at a repetition rate of $f=1\text{kHz}$. The polarised beam optionally passes a SHG frequency conversion with a $500\mu\text{m}$ thin BBO crystal. Afterwards the beam is transferred into a NC controlled positioning stage with three perpendicular translational axes with an absolute accuracy of 100nm and a repeatability of 250nm . The laser radiation is focused to a calculated spot size of about $1\mu\text{m}$ by a microscope objective, either with a magnification of $50\times$ and a NA of 0.55 or a magnification $63\times$ and a NA of 0.7 . The applied pulse energy is adjusted so that the fluence is at the ablation threshold for each material. Ablation threshold is defined as the fluence where the first changes of the surface are detectable by microscopy. The pulse energy is determined directly in front of the microscope objective.

The samples are processed by scanning the focused laser radiation over the surface. For ripple formation, a scanning speed is chosen in the way that the pulse spacing d (distance between two successive pulses) is smaller or equal to 200nm for structures made with a wavelength of $\lambda=800\text{nm}$, resulting in an overlap of at least 80% . Due to a slightly smaller ablation diameter for structures made with $\lambda=400\text{nm}$ the pulse spacing is chosen smaller or equal to 100nm . These limitations for the pulse spacing are selected, because the ripple spacing Λ for fused silica does not depend on the pulse spacing for more than two orders of magnitude ($d=1-10^2\text{nm}$) [24]. But the spacing Λ rises linearly when the pulse spacing exceeds about one third of the focus diameter, because then no more ripples emerge, but the single successive pulses become visible [24].

All experiments were performed in ambient air at normal incidence.

After being cleaned in an ultrasonic bath of pure ethanol, the samples are sputter coated with a thin film of gold and investigated by scanning electron microscopy (SEM) to determine lateral dimensions on the surface. For each material numerous line scans are measured over contiguous ripple patterns to determine the ripple spacing and its statistical error (standard deviation).

3. Results

Ripples structures with spacing significantly smaller than the irradiation wavelength are observed on all the samples (fig. 1-3). The clarity of contour and edges of the linear structures depend on the material (fig. 2). Ripple spacings from 139nm to 532nm are detected (tab. 1) depending on the material and the wavelength. The direction of the resulting grooves is perpendicular to the polarisation of the laser radiation. The ripples extend coherently regardless of the orientation of the scanning over many partially overlapping laser pulses; hence a change of the scanning direction does not change the orientation of the ripples (fig. 1). A scanning perpendicular to the polarisation results in long parallel grooves (fig. 3).

The ripple spacing for one material does not distinctly differ for the two used microscope objectives, but depends on the applied wavelength (tab. 1). In some cases the ripples are surrounded by a small amount of deposit of ablated material (fig. 2).

The investigated materials include transparent dielectrics (SiO₂, LiF, MgF₂, Al₂O₃, ZBLAN), a non transparent polymer (PTFE) and a non-transparent semiconductor (Si). All materials exhibit ripples after processing. The ripple spacing Λ is increasing in the mentioned order of materials for an applied wavelength of 800nm . The ripple spacing for the semiconductor silicon $\Lambda_{\text{Si},800\text{nm}}=(532\pm62)\text{nm}$ is the highest among the measured. The values of the ZBLAN $\Lambda_{\text{ZBLAN},800\text{nm}}=(312\pm24)\text{nm}$ and polymer $\Lambda_{\text{PTFE},800\text{nm}}=(338\pm21)\text{nm}$ are situated between the one for silicon and the other transparent dielectrics that range from 189 to 276nm for $\lambda=800\text{nm}$.

For LiF a reduction of the applied wavelength from $\lambda=800\text{nm}$ to 400nm results in a decrease of the ripple spacing by a factor of about 1.6, from $\Lambda_{\text{LiF},800\text{nm}}=(215\pm 37)\text{nm}$ to $\Lambda_{\text{LiF},400\text{nm}}=(139\pm 18)\text{nm}$. Scanning the focus once perpendicular to the polarisation results in long parallel grooves with a very clear contour and sharp edges, a width of about 125nm and a spacing of about 240nm (fig. 3). For a focus with a diameter of about $1\mu\text{m}$ on ZBLAN two grooves are formed, but in general the number of grooves depends on the diameter of the focus. The edges of these structures are excellent with respect to the applied wavelength, but are not expected to have a high aspect ratio depth over width.

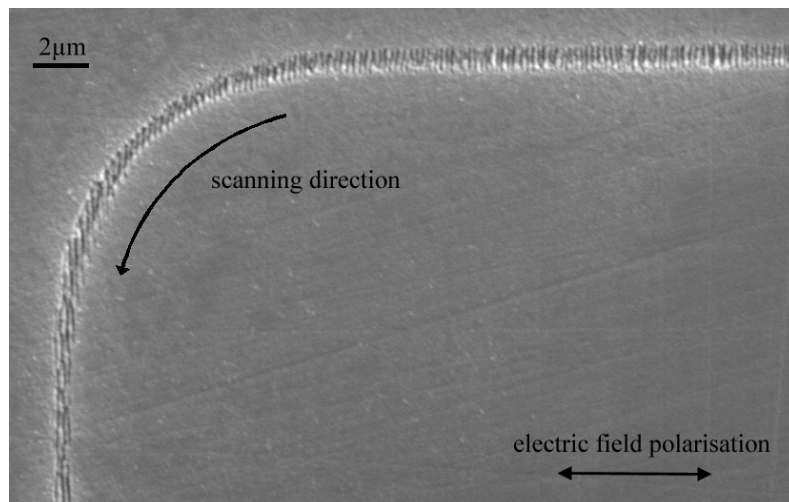


Figure 1. Ripples in Al_2O_3 with changing scanning direction (SEM), $\lambda=800\text{nm}$, $t_p=100\text{fs}$, $f=1\text{kHz}$, $d_{\text{pulse}}=20\text{nm}$.

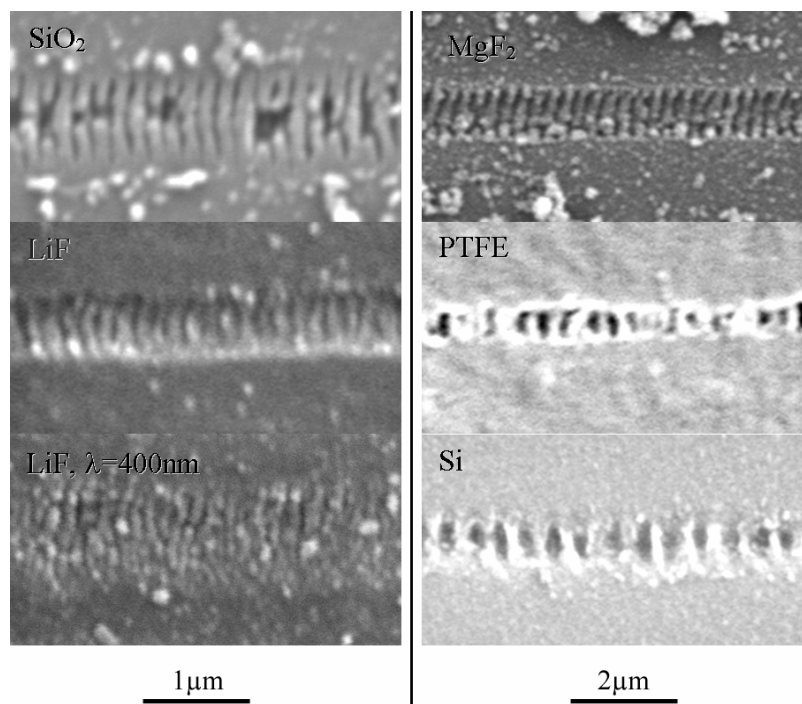


Figure 2. Ripples in SiO_2 , LiF, MgF_2 , PTFE & Si with scanning direction parallel to the polarization (SEM), $\lambda=800\text{nm}$ (except as indicated), $t_p=100\text{fs}$, $f=1\text{kHz}$. All pictures on the left hand side have a $1\mu\text{m}$ scale, all on the right hand side show two times wider segments of the samples.

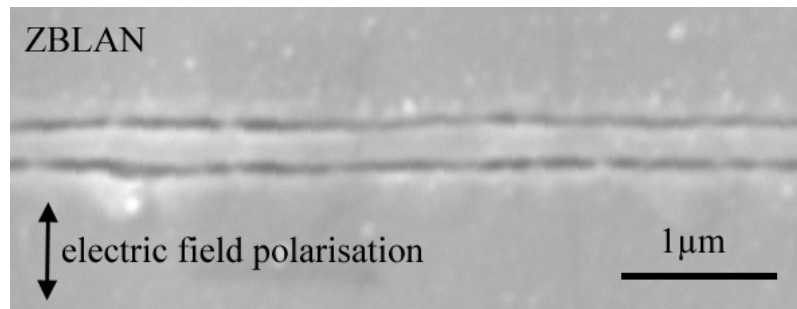


Figure 3. Ripples in ZBLAN with scanning direction perpendicular to the polarization (SEM), $\lambda=800\text{nm}$, $t_p=100\text{fs}$, $f=1\text{kHz}$.

Table 1. Ripples in various materials (SEM), $t_p=100\text{fs}$, $f=1\text{kHz}$

| material | wavelength (nm) | ripple spacing (nm) | error (nm) |
|--------------------------------|-----------------|---------------------|------------|
| SiO ₂ | 800 | 189 | 29 |
| LiF | 800 | 215 | 39 |
| LiF | 400 | 139 | 18 |
| MgF ₂ | 800 | 235 | 27 |
| Al ₂ O ₃ | 800 | 276 | 38 |
| ZBLAN | 800 | 312 | 24 |
| PTFE | 800 | 338 | 21 |
| Si | 800 | 532 | 62 |

4. Discussion

All the measured ripple spacings are significantly below the wavelength of the laser radiation used. The smallness of the ripple spacing in relation to the applied wavelength can not be explained in scope of the classical theory [2] by an inclination of the beam, because of the perpendicular incidence during the preparation of the presented ripples. The ripple spacing, however, depends on the irradiated material, probably due to materials properties like refractive index or/and band gap. Thereby it has to be paid regard that high-intensity femtosecond light pulses change the initial optical properties e.g. the refractive index during and some time after the pulse, due to the generation of free electrons [25].

The classical theory of ripple formation [2, 3] has a good accuracy in forecasting ripple formation for non ultra short pulsed laser radiation, so a first appropriate procedure is to supplement the theory with characteristics of the interaction of femtosecond laser radiation with matter. Therefore, a preliminary explanation for the formation of the material dependent sub-wavelength ripples formation is the interaction of the incident wave with surface electromagnetic waves (SEW) [26] (e.g. plasmons [27, 28]) additionally taking into account multi-photon processes and the change of material properties due to the high intensity during pulse. The free electrons density typically created by the fs-pulse is large enough to make semiconductor or metal like behaviour possible, and thereby should allow plasmons on the surface of dielectrics. The dependence of the ripple spacing on the materials properties indicates that the involved SEW is travelling inside the material and not above.

5. Conclusion

Formation of sub-wavelength ripples from $\Lambda \approx 1/4 \cdot \lambda$ to $3/4 \cdot \lambda$ in a focus diameter of $\sim 1 \mu\text{m}$ by femtosecond laser radiation has been shown for two different wavelength on divers materials. The ripples extend coherently regardless of the orientation of scanning.

In opposition to the classical ripple theory, the ripple spacing is clearly dependent on the materials properties, giving indication to understand the processes during the sub-wavelength ripple formation by femtosecond laser radiation.

Concerning possible applications the structuring with a scanning direction parallel to the ripple orientation (fig. 3) proved to be beneficial for the production of waveguides in thin films [23] due to the resulting smooth edges.

References

- [1] M. Birnbaum, *J. Appl. Phys.* 36, **3688** (1965)
- [2] Z. Guosheng, P. M. Fauchet, A. E. Siegman, *Phys. Rev. B* 26 (10) **5366** (1982)
- [3] J. E. Sipe, J. F. Young, J. S. Preston, H. M. van Driel, *Phys. Rev. B*, 27 (2) **1141** (1983)
- [4] A. Barborica, I. N. Milhailescu; V. S. Teodorescu, *Phys. Rev. B*, 49(12), **8385** (1994)
- [5] D. C. Emmony, R. P. Howson, L. J. Willis, *Appl. Phys Lett.* 23(11), **598** (1973)
- [6] G. N. Maracas, G. L. Harris, C. A. Lee, R. A. McFarlane, *Appl. Phys. Lett.* 33(5) **453** (1978)
- [7] N. R. Isenor, *Appl. Phys. Lett.* 31(3) **148** (1977)
- [8] D. Bäuerle: Laser processing and chemistry, Springer-Verlag, Berlin Heidelberg New York, 2nd Edition (1996)
- [9] Y. F. Lu, W. K. Choi, Y. Aoyagi, A. Kinomura, K. Fujii, *J. Appl. Phys.* 80(12) **7052** (1996)
- [10] M. Oron, G. Sørensen, *Appl. Phys. Lett.* 35(10) **782** (1979)
- [11] P. Tosin, A. Blatter, W. Lüthy, *J. of Appl. Phys.* 78(6) **3797-3800** (1995)
- [12] V. P. Aksenov, SPIE Vol 473 *Symposium OPTIKA '84*, **294** (1984)
- [13] J. Gottmann, G. Schlaghecken, R. Wagner, E. W. Kreutz, Fabrication of erbium doped planar waveguides by pulsed laser deposition and laser micromachining. Proc. SPIE from EPF 2002, 4941, **148-156** (2003)
- [14] B. N. Chichkov, C. Momma, S. Nolte, F. von Alvensleben, A. Tünnermann, *Phys. Rev. A* 63, **109** (1996)
- [15] D. Ashkenasi, A. Rosenfeld, H. Varel, M. Wähmer, E. E. B. Campbell, *Appl. Surf. Sci.* 120 **65-80** (1997)
- [16] J. Bonse, S. Baudach, J. Krüger, W. Kautek, M. Lenzner, *Appl. Phys. A* 74 **19-25** (2002)
- [17] H. Varel, M. Wärmner, A. Rosenfeld, D. Ashkenasi, E. E. B. Campbell, *Appl. Surf. Sci.* 127-129, **128-133** (1998)
- [18] A. M. Ozkan, A. P. Malshe, T. A. Railkar, W. D. Brown, M. D. Shirk, P. A. Molian, *Appl. Phys. Lett.* 75 (23), **3716** (1999)
- [19] Q. Wu, Y. Ma, R. Fang, Y. Liao, Q. Yu, X. Chen, K. Wang, *Appl. Phys. Lett.* 82(11), **1703** (2003)
- [20] A. Borowiec, H. K. Haugen, *Appl. Phys. Lett.* 82 (25) **4462** (2003)
- [21] N. Yasumaru, K. Miyazaki, J. Kiuchi, *Appl. Phys. A* 76, **983** (2003)
- [22] F. Costache, M. Henyk, J. Reif, *Appl. Surf. Sci.* 208-209, **486** (2003)
- [23] P. Rudolph; W. Kautek, *Thin Solid Films* 453-454 **537-541** (2004)
- [24] R. Wagner, J. Gottmann, Alexander Horn, Ernst W. Kreutz, Proc. SPIE from LPM2004, 5662, **168** (2004)
- [25] A. M. Streltsov, J. K. Ranka, A. L. Gaeta, *Optics Letters* 23 (10), 798 (1998)
- [26] A. V. Andreev, M. M. Nazarov, I. R. Prudnikov, A. P. Shkurinov, P. Masselin, *Phys. Rev. B* 69 035403-1 (2004)
- [27] J. M. Elson, R. H. Ritchie, *Phys. Stat. sol. (b)* 62, 461 (1974)
- [28] J. M. Pereira Jr., G. A. Farias, R. N. Costa Filho, *Eur. Phys. J. B* 36, 137-140 (2003)